of the apocrine lesion, size, presence of necrosis and calcifications, hormone receptor status, cytoplasmic and nuclear features. The association of these features with upgrade rates was examined for statistically significant findings.

Results: A total of 46 cases of atypical apocrine lesions, including atypical apocrine adenosis and apocrine atypical ductal hyperplasia, were included in the study. The average size of atypical apocrine lesions was 1.9 mm. A solid pattern was present in 22 cases (48%), cribriform in 19 (41%), papillary in 8 (17%), micropapillary in 4 (9%), and lobular involvement in 17 cases (37%). The nuclei were slightly enlarged (<2x background) in 19 cases (41%), enlarged (2x background) in 12 cases (26%), and markedly enlarged (>2x background) in 15 cases (33%). Nucleoli were absent in 2 cases (4%), vague in 7 (15%), slightly obvious in 7 (15%), obvious in 25 (54%), obvious with some pleomorphism in 2 (4%), and pleomorphic in 3 cases (7%). Histologic features of atypical apocrine lesions are summarized in Table 1. Interestingly, obvious nucleoli were significantly more present in cases with DCIS upgrades on follow-up excision compared to those without DCIS upgrades (7/7 vs. 22/39; $p<0.05$). A cribriform pattern was significantly more common in cases upgraded to invasive carcinoma compared to those without an invasive upgrade (3/3 vs. 16/43; $p<0.05$).

Conclusions: Our study suggests that breast cases with atypical apocrine lesions featuring obvious nucleoli are associated with DCIS on excision, while the cribriform pattern is associated with an upgrade to invasive carcinoma. These histologic features may be valuable in identifying patients with atypical apocrine lesions who are at high risk of in-situ or invasive carcinoma.

Table 1
Summary of histologic features of atypical apocrine lesions.

	Number of Cases (Percent of Total)
Average Size	1.9 mm
Pattern	
Solid	22 (48%)
Cribriform	19 (41%)
Papillary	8 (17%)
Micropapillary	4 (9%)
Lobular Extension	17 (37%)
Nuclear Size	
<2x background	19 (41%)
2x background	12 (26%)
>2x background	15 (33%)
Nucleoli	
Absent	2 (4%)
Vague	7 (15%)
Slightly Obvious	7 (15%)
Obvious	25 (54%)
Obvious With Some Pleomorphism	2 (4%)
Pleomorphic	3 (7%)
Necrosis	2 (4%)
Calcifications	16 (35%)

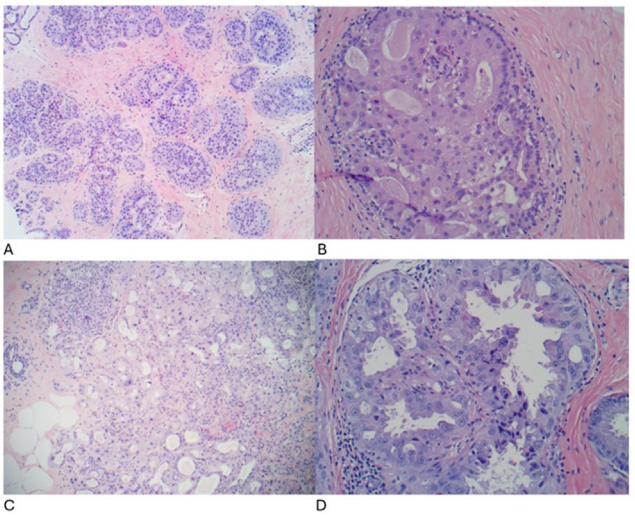

Figure 1: Examples of atypical apocrine lesions with predominantly solid pattern (A), cribriform pattern (B), marked nuclear pleomorphism (C), and prominent nucleoli (D).

Figure 1 - 214.

Lab Invest 105 (2025) 102438

https://doi.org/10.1016/j.labinv.2024.102438

215 | Enhancing Precision Oncology for Haitian Breast Cancer Patients Using Deep Learning-Enabled Histopathology Analysis

Dagoberto Pulido Arias[1], Rebecca Henderson[2], Gabriel Flambert[2], Michael Mathelier[2], Maisha Corrielus[2], Tiago Gonçalves[3], Elizabeth Gerstner[4], Kenneth Landgraf[5], Jose Jeronimo[6], Philip Castle[6], Jane Brock[7], Christopher Bridge[4], Albert Kim[8], Lormil Joarly[9], Christophe Millien[9], Marie Jose[9], Jean Bontemps[2], [1] *Mass General Brigham, Boston, MA;* [2] *University of Florida, Gainesville, FL;* [3] *Porto, Portugal;* [4] *Mass General Brigham, Harvard Medical School, Boston, MA;* [5] *American Society for Clinical Pathology (ASCP), Chicago, IL;* [6] *National Institute of Health, Bethesda, MD;* [7] *Worcester, MA;* [8] *Massachusetts General Hospital, Harvard Medical School, Boston, MA;* [9] *Boston, MA*

Disclosures: Dagoberto Pulido Arias: None; Rebecca Henderson: None; Gabriel Flambert: None; Michael Mathelier: None; Maisha Corrielus: None; Tiago Gonçalves: None; Elizabeth Gerstner: None; Kenneth Landgraf: None; Jose Jeronimo: None; Philip Castle: None; Jane Brock: None; Christopher Bridge: None; Albert Kim: None; Lormil Joarly: None; Christophe Millien: None; Marie Jose: None; Jean Bontemps: None

Background: Deep learning (DL)-based computer vision analysis has shown promise in identifying therapeutically relevant biology within conventional histopathology (H&E). Given the lack of pathology resources in lower-middle income countries (LMICs), DL-enabled H&E analysis can facilitate precision-based care for LMIC patients. However, most DL models have been trained using data from a predominantly European population and will likely not generalize to LMIC patients. To this end, we have curated a dataset of 3000 H&E WSIs from Zanmi Lasante (Haiti) with paired estrogen-receptor (ER) status.

Design: Using The Cancer Genome Atlas (TCGA) breast cancer and Zanmi Lasante datasets, we developed a DL-based ER classification tool, using H&E whole slide images (WSIs), for Haitian breast cancer patients. ER status is needed to identify patients who would benefit from endocrine therapy. However, ER determination is not always possible in LMIC, given the lack of resources for immunohistochemistry. As the TCGA dataset is predominantly comprised of patients of European ancestry, we assessed whether a TCGA-trained model would generalize to Haitian patients. After WSI processing and feature extraction, attention-based weakly

supervised multiple instance learning (ABMIL) was used to train a classification model. To assess performance, both the TCGA and Zanmi Lasante datasets were split into training (70%), validation (15%), and testing (15%) sets, and the results were compared across both patient populations.

Results: Our TCGA-trained classification model demonstrated a performance of an area under receiver operating characteristic (AUROC) of 0.92 on the "held-out" TCGA test set and an AUROC of 0.71 on the Haitian "held-out" test set for the prediction of ER+ status. This domain shift is consistent with known biological differences between tumor samples of European and Black breast cancer patients. Notably, pre-training a model on the TCGA dataset and fine-tuning on the Haitian dataset improved predictive performance substantially to an AUROC of 0.80.

Pretrain dataset	Train Set	Test Set (Held-out)	AUC
	TCGA	TCGA	0.92
	Haiti (3,000 images)	Haiti	0.79
	TCGA	Haiti	0.73
	Haiti (1,000 images)	Haiti	0.71
TCGA	Haiti (1,000 images)	Haiti	0.80

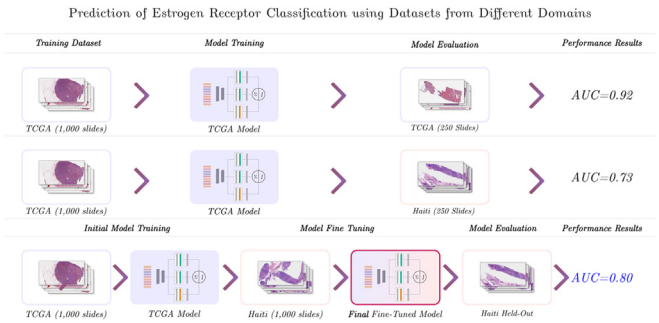

Figure 1 - 215.

This study illustrates the potential of DL to advance precision medicine in low-resource settings, and highlights a need for adequate training data from LMIC patients. By addressing these domain gaps, we can develop more generalizable DL models to diverse patient populations. This work will serve as a starting point for new collaborations with global LMIC pathologists and oncologists.

Lab Invest 105 (2025) 102439
https://doi.org/10.1016/j.labinv.2024.102439

216 | Can Magee Equations Predict Extent and Pattern of Response to Neoadjuvant Chemotherapy in Hormone-Positive Breast Cancers

Sumaira Qayoom[1], Shehla Fayyaz[1], Naseem Akhtar[1], Pooja Ramakant[1], Mala Sagar[1], Shiv Rajan[1], Vidya Rashmi[1], [1] *King George's Medical University, Lucknow, India*

Disclosures: Sumaira Qayoom: None; Shehla Fayyaz: None; Naseem Akhtar: None; Pooja Ramakant: None; Mala Sagar: None; Shiv Rajan: None; Vidya Rashmi: None

Background: In Breast cancer, Magee Equations (ME) have been proposed as a surrogate of Oncotype Dx to predict the recurrence score and were further evaluated to predict the response to chemotherapy. Predicting the type of response and pattern of residual tumor in patients who do not show pathologic complete response (pCR) has clinical implications. This study aims to evaluate the chemo-predictive role of Magee Equations and their relationship to residual tumor patterns.

Design: Eighty-five hormone-positive non-metastatic breast cancer cases were prospectively included between April 2023 and June 2024. Magee Equations (ME1, ME2, ME3) were calculated on pre-therapy core biopsy using an online calculator https://path.upmc.edu/onlineTools/mageeequations.html. Magee score <25 was considered low and >25 as high. pCR, as defined by CAP guidelines, was considered the primary endpoint. Residual Cancer burden (RCB) was calculated using MD Anderson's online calculator. Residual tumor response was classified as concentric and scattered and further categorised into four patterns (A-D) based on tumor cell distribution and intervening fibrosis. All three Magee scores were correlated with residual cancer burden, type and pattern of response.

Results: pCR was seen in 20 (23.5%) cases, residual cancer burden was classified as RCBII in 46 (54.1%) cases and RCBIII in 19 (22.4%) cases. Among 65 cases with residual disease, 27 (41.5%) cases had a concentric response, while 38 (58.5%) showed a scattered pattern**.** Pattern C was the most common residual tumor pattern seen in 25 (38.5%), followed by Pattern B in 20 (30.8%). High Magee scores (>25) were significantly associated with pCR(P<0.05), with ME3 showing the strongest correlation. No significant association was found between Magee scores and residual tumor patterns.

Table 1
Association of Magee scores with Residual Cancer Burden, type and pattern of response to Neoadjuvant chemotherapy.

Magee Score	Residual cancer burden				p-Value	Type of response		p- Value	Pattern of response				P-Value
	pCR	RCB I	RCB II	RCB III		Concentric	Scattered		A	B	C	D	
Magee 1	8 (15.1)	0	27 (50.9)	18 (34.0)	**0.001**	16 (35.6)	29 (64.4)	**0.142**	5 (11.1)	12 (26.7)	19 (42.2)	9 (20.0)	**0.716**
Low (n=53)	12 (37.5)	0	18 (34.0)	1 (3.1)		11 (55.0)	9 (45.0)		2 (10.0)	8 (40.0)	6 (30.0)	4 (20.0)	
High (n=32)													
Magee 2	9 (16.7)	0	28 (51.9)	17 (31.5)	**0.013**	16 (35.6)	29 (64.4)	**0.142**	5 (11.1)	12 (26.7)	18 (40.0)	10 (22.2)	**0.737**
Low (n=54)	11 (35.5)	0	18 (58.1)	2 (6.5)		11 (55.0)	9 (45.0)		12 (26.7)	8 (40.0)	7 (35.0)	3 (15.0)	
High (n=31)													
Magee 3	8 (14.3)	0	30 (53.6)	18 (32.1)	**0.001**	18 (37.5)	30 (62.5)	**0.267**	5 (10.4)	14 (29.2)	19 (39.6)	10 (20.8)	**0.960**
Low (n=56)	12 (41.4)	0	16 (55.2)	1 (3.4)		9 (52.9)	8 (47.1)		2 (11.8)	6 (35.3)	6 (35.3)	3 (17.6)	
High (n=29)													
Av. Magee	8 (15.1)	0	27 (50.9)	18 (34.0)	**0.001**	16 (35.6)	29 (64.4)	**0.142**	5 (11.1)	12 (26.7)	18 (40.0)	10 (22.2)	**0.737**
Low (n=53)	12 (37.5)	0	19 (59.4)	1 (3.1)		11 (55.0)	9 (45.0)		2 (10.0)	8 (40.0)	7 (35.0)	3 (15.0)	
High(n=32)													